# *On the Formation of Ammonium Nitrate from the Thermal Decomposition of Hydroxylammonium Nitrate: Quantification of $NH_3$ and $HNO_3$*

N.R. Taylor and K.M. Lemmer
Western Michigan University
Kalamazoo, MI

## ABSTRACT

The ionic liquid hydroxylammonium nitrate (HAN) is a promising propellant for various types of spacecraft propulsion including chemical monopropellants, electrospray thrusters, and field reversed configuration thrusters. In order to maximize the efficiency of the propellant, knowledge of its physical and chemical characteristics under conditions similar to those utilized for spacecraft propulsion is required. An experimental platform has been developed to deliver a controlled flow of HAN through a heated stainless-steel capillary for thermal decomposition under vacuum conditions. The resulting vaporized species immediately flow through a fused quartz tube maintained at a base pressure of approximately 65 mTorr. Upon initial examination of the experimental platform, it was discovered that an unknown white solid would develop on the surface of the quartz tube when HAN was thermally decomposed in the absence of a plasma. A full spectroscopic analysis was conducted on the unknown solid which included Raman spectroscopy, FT-IR spectroscopy, NMR spectroscopy, and pH analysis. From these data it was concluded that the unknown solid was pure ammonium nitrate ($NH_4NO_3$) and likely formed from the production of ammonia, $NH_3$, and nitric acid, $HNO_3$. Based on this discovery, we subsequently undertook a quantitative study of the production of $NH_3$ due to HAN decomposition. Known quantities of HAN were thermally decomposed, resulting in the deposition of solid $NH_4NO_3$ on the quartz tube, which was collected and analyzed via Raman spectroscopy. This approach facilitated direct quantification of $NH_3$. By adding additional $NH_3$ to the system, nitric acid could also be quantified. Parameters examined include thermal decomposition temperature and HAN injection flow rate.

## INTRODUCTION

Ionic liquids (ILs) have emerged in recent years as potential “green” monopropellants for chemical propulsion with interest in a dual-mode propellant replacement in electric propulsion devices.[1,2] In addition to being environmentally benign, ILs tend to be chemically stable and exhibit low-toxicity. Due to very strong intramolecular interactions (ion-dipole, dipole-dipole, and hydrogen bonding) IL densities are relatively high and their vapor pressures are extremely low. As a result they have been widely utilized as propellants in electrospray thrusters.[3–12] Moreover, ILs are known to thermally decompose into gas phase species which can be utilized as the feed gas in gas-fed electric propulsion devices.[2,13–31] In order to maximize the propellant’s utility, the parameters that influence chemical composition of the emitted gas phase species must be well characterized.

One particular IL that has received notable attention is hydroxylammonium nitrate (HAN). In 1986 Cronin and Brill examined the decomposition of HAN and speculated that the initial reaction involved proton transfer from the hydroxylammonium ion ($NH_3OH^+$) to the nitrate ion ($NO_3^-$) to form hydroxylamine ($NH_2OH$) and nitric acid ($HNO_3$).[31] They postulated that hydroxylamine would further degrade into nitrous oxide ($N_2O$) and ammonia ($NH_3$). Interestingly, they also noted the possibility that ammonium nitrate ($NH_4NO_3$) would form due to the generation of ammonia and the vaporization of nitric acid. More recently Chambreau *et al.* examined the thermal decomposition of HAN under vacuum conditions and conclusively demonstrated the formation of ammonia as well as vaporized nitric acid, although quantitative measurements were not reported.[32]



Air Force Office of Scientific Research Grant FA9550-18-1-0442

In recent years there have been a number of computational studies examining the decomposition of hydroxylamine.[33–35] Most notable is the extensive study conducted by Izato *et al.* where they examined the early decomposition pathways of hydroxylamine in aqueous solutions.[34] Based on their computational analysis they concluded that a cation-catalyzed reaction was the likely initial decomposition pathway, as shown in reactions R1-R6, with R6 being the overall reaction.

R1. $NH_3OH^+ + NO_3^- \rightarrow NH_2OH + HNO_3$

R2. $NH_2OH + NH_2OH + NH_3OH^+ \rightarrow NH_2NH_2OH^+ + NH_2OH + H_2O$

R3. $NH_2NH_2OH^+ \rightarrow NH_3NH_2O^+$

R4. $NH_3NH_2O^+ \rightarrow NH_4^+ + HNO$

R5. $NH_4^+ + NH_2OH \rightarrow NH_3OH^+ + NH_3$

**R6.** $\mathbf{NH_2OH + NH_2OH \rightarrow NH_3 + HNO + H_2O}$

Based on these experimental and computational reports, it is reasonable to conclude that the formation of ammonia and nitric acid from the thermal decomposition of HAN would lead to the formation of ammonium nitrate; however, to our knowledge this observation has not been reported. Therefore, the objective of this research is to first experimentally verify that ammonium nitrate is produced from the thermal decomposition of HAN. This will be accomplished by decomposing HAN under a controlled set of conditions and collecting the solid material generated. A complete chemical analysis of this solid material will be conducted which will include Raman, NMR, FT-IR, and pH analysis. Secondly, we will examine the experimental conditions in which HAN undergoes partial and total thermal decomposition within an actively controlled flowing thermal capillary system. Analysis of Raman spectra acquired from the HAN decomposition material collected under a series of temperatures and flow rates is used to assess the degree to which HAN decomposes. Finally, the formation of ammonium nitrate will be used to quantify the amount of ammonia and nitric acid generated relative to the amount of injected HAN. The results obtained from this research effort will aid in the validation of computational modeling efforts as well as assist application researchers in the optimization of gas-phase electric propulsion thruster designs which utilize HAN as a propellant.

## EXPERIMENTAL DESIGN

An illustration of the experimental system used to examine the production of ammonia and nitric acid is shown in figure 1. Controlled quantities of HAN are injected into the thermal decomposition system by controlling the pressure differential between the vacuum chamber and liquid reservoir. The thermal decomposition system was evacuated to a base pressure of 65 mTorr and the pressure exerted on the liquid reservoirs was controlled with a mass flow controller. The mass flow controller allows direct control of the back pressure exerted on the liquid reservoirs, facilitating active control of the liquid flow rate through the system. An automated 3-way valve is used to select between the HAN reservoir or the $H_2O$ reservoir which was used for flushing the system. A liquid flow meter positioned in-line with the capillary system is used to measure the flow rate of liquid delivered to the thermal decomposition system. The liquid emerging from the flow meter flows through a fused silica capillary with an inner diameter of 25 μm which restricts flow and allows more precise control of the flow rate. The resulting liquid is injected into a stainless-steel capillary with an inner diameter of 178 μm (0.007”), an outer diameter of 4.76 mm (3/16”), and a length of 200 mm. The final 50 mm portion of the stainless-steel capillary is confined within an aluminum heating block at a temperature controlled with thermal tape. Four embedded K-type thermocouples positioned along the heating block (only one shown) acquire temperature measurements along the heated portion of the capillary. Immediately following the end of the heated capillary are two sintered stainless-steel disks. The first disk has a



Air Force Office of Scientific Research Grant FA9550-18-1-0442

porosity of 100 μm, and the second disk has a porosity of 10 μm. The purpose of the stainless-steel disks is to homogenize the gas vapor that emerges from the capillary; thus, providing a fairly uniform distribution of vaporized species. An additional feature of these metal disks is the potential for catalytic studies; although, no catalytic studies have been conducted with this experimental setup. The gas vapor emerging from the metal disks flows through an 8" long fused quartz tube with an outer diameter of 25.8 mm and an inner diameter of 22 mm. The end of the fused quartz tube has been tapered to a final inner diameter of 5 mm for purposes of subsequent laser-induced fluorescence studies. Approximately 50 mm of the quartz tube is inserted into the heating block and vacuum sealed with high temperature O-rings. The remaining 150 mm tube is exposed to the ambient lab environment and provides an ideal cool surface on which the generated ammonium nitrate can condense; thus, providing a means to collect any ammonium nitrate generated from the decomposition of HAN.

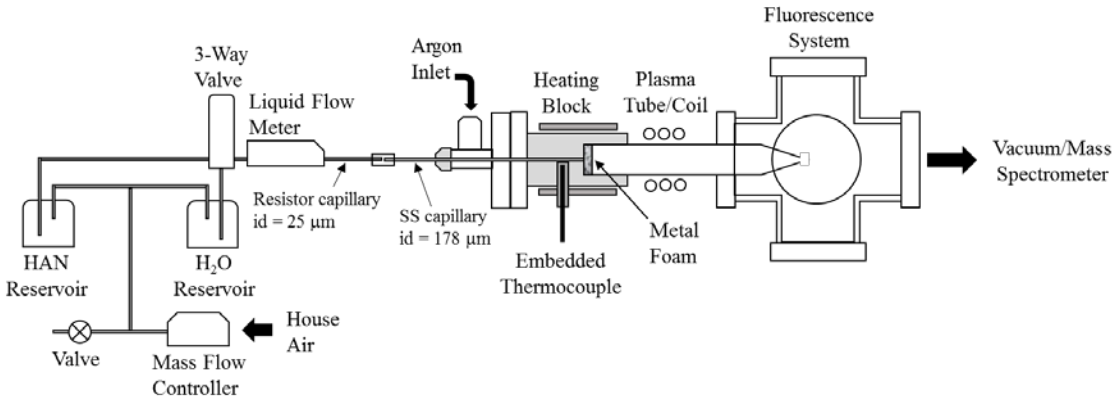


Figure 1: Illustration of the experimental platform used for thermal decomposition and plasma excitation of ionic liquid propellants.

In the sections below, the experimental methods for each experiment are discussed in detail. Briefly, Raman spectroscopy, pH analysis, Nuclear Magnetic Resonance Spectroscopy, and Fourier Transfer Infrared Spectroscopy were performed on the unknown solid.

## RESULTS AND DISCUSSION

The formation of ammonia and nitric acid via thermal decomposition of HAN will remain in the gas phase until these molecules are sufficiently cooled and allowed to condense on a surface. The quartz tube, which will be utilized in subsequent plasma-based studies provides a convenient surface on which the generated ammonium nitrate can deposit and subsequently be collected. Initial experiments were conducted to verify that the material collected was composed of ammonium nitrate. HAN was injected into the system at a flow rate of approximately 50 nL/s and a decomposition temperature of 440 K. As shown in figure 2, a white solid developed on the surface of the quartz tube, with a bulk of the solid formation occurring at a distance of approximately 25 mm downstream from the heating block. Temperature measurements on the exterior surface of the quartz tube indicated that the onset of solid deposition occurred at a temperature of approximately 323 K (50 °C). No observed material was deposited on the final 50 mm of the tube, indicating that all of the ammonium nitrate formed was deposited on the tube's surface. Upon completion of the HAN decomposition, the quartz tube was removed, and the material was collected and stored in a test tube for subsequent

Figure 2: Image of the plasma tube with a white solid deposited on the inner surface due to HAN decomposition.



Air Force Office of Scientific Research Grant FA9550-18-1-0442

spectroscopic analysis. For clarity, the collected solid material from the decomposition of HAN will be referred to as the unknown, while prepared standards of ammonium nitrate used for analytical comparison will simply be referred to as ammonium nitrate

## RAMAN SPECTROSCOPY

A portion of the collected unknown white solid was initially dissolved in water to a concentration of 3.52% (wt.) and subsequently analyzed by Raman spectroscopy. The Raman spectroscopic system consisted of a single mode dye laser at 578.844 nm, with a linewidth of ~250 kHz and an output power of 1.5 W. The resulting Raman photons were collected with a series of lenses and detected with a high-resolution spectrometer equipped with a cooled CCD detector. The spectrometer was wavelength calibrated with an Hg/Ar calibration standard. Furthermore, the spectral responsivity of the spectrometer was calibrated with a NIST traceable spectral irradiance source. A series of standards were examined in concert with the unknown sample for comparison, with results shown in figure 3. These spectra have been background corrected and normalized to the 1076.6 $cm^{-1}$ peak except for the $H_2O$ spectrum which was simply scaled for visual comparison.

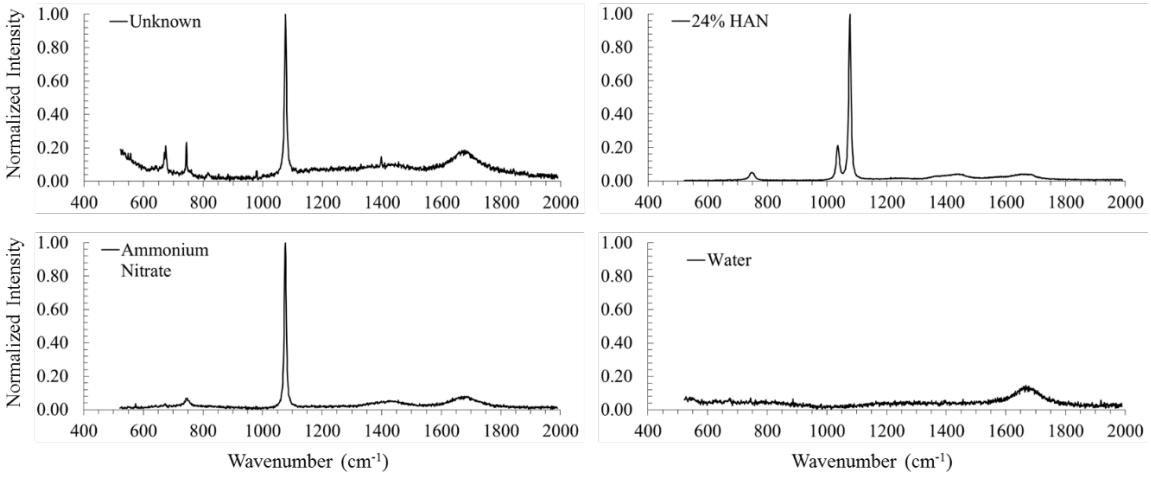


Figure 3: Raman spectra of the unknown white solid in an aqueous solution at a concentration of 3.52% (wt.), aqueous solution of HAN at a concentration of 24% (wt.), aqueous solution of ammonium nitrate at a concentration of 7.05% (wt.), and pure water.

Based on the initial Raman data shown in figure 3 two determinations can be formed. First, the unknown HAN decomposition product is not composed of solidified hydroxylammonium ($NH_3OH^+$) or hydroxylamine ($NH_2OH$) due to the absence of the signature N-OH vibrational mode at 1035.5 $cm^{-1}$, which is clearly present in the 24% HAN spectrum.[17] The second determination we can make is that the unknown contains a nitrate ion, $NO_3^-$, due to the N=O symmetric stretching mode at 1076.6 $cm^{-1}$, which is consistent with each of the nitrate containing species examined in figure 3. The Raman spectra of the unknown collected solid is consistent with the production of ammonium nitrate; however, further analysis is required for identification confidence.

## PH ANALYSIS

While pH measurements are generally not useful for compound identification, they can be useful in reducing the number of possible species and adding complimentary experimental evidence in support of the conclusion from the spectroscopic analysis. A standard laboratory pH probe calibrated with a pH = 4 standard buffer solution was used to measure the pH of the



Air Force Office of Scientific Research Grant FA9550-18-1-0442

unknown aqueous solution, which was found to be 4.79. If the unknown were assumed to be ammonium nitrate ($NH_4^+$ $pK_a$ = 9.25), the unknown would have a calculated pH of 4.80. Although this analysis is not conclusive, the result is consistent with the unknown substance possessing an ammonium ion.

## NUCLEAR MAGNETIC RESONANCE SPECTRSCOPY

Nuclear magnetic resonance spectroscopy (NMR) has historically been the analytical mainstay for synthetic chemists, as well as biologists, for molecular structure determinations. Therefore, acquiring a proton NMR spectra would provide conclusive evidence to support the presence of an ammonium ion within the unknown solid. The unknown solid was dissolved in deuterated water ($D_2O$ = 99.96%) to a concentration of 0.65 M. A small amount of nitric acid was also added to the solution to reduce the pH in order to shift the equilibrium to favor the formation of an ammonium ion over its conjugate base, ammonia ($NH_3$). Furthermore, an ammonium nitrate standard was prepared in a similar way, with a concentration of 1.25 M. These solutions were analyzed with a 400 MHz NMR equipped with an auto-sampler. The resulting proton NMR spectra are shown in figure 4.

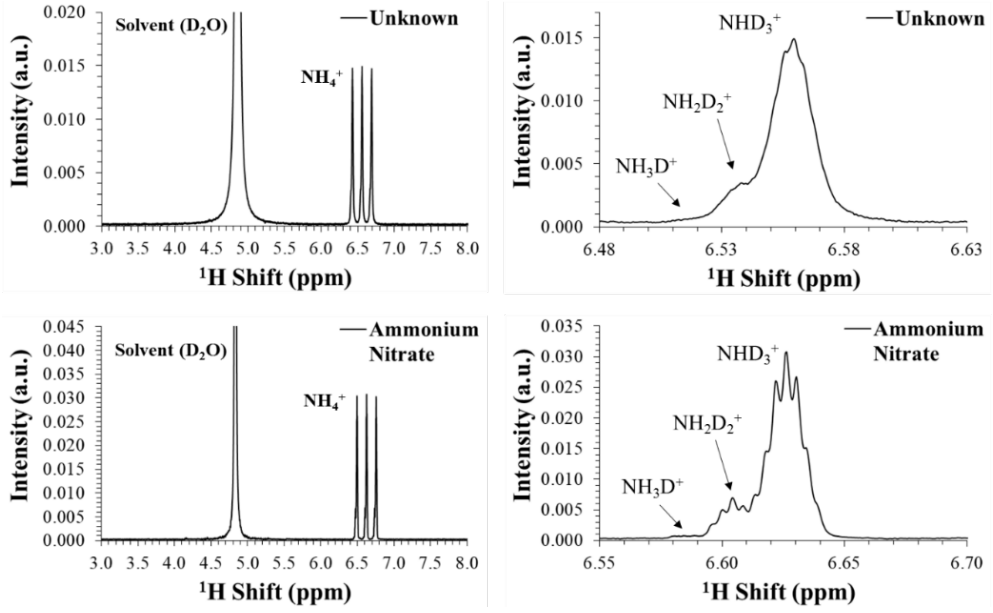


Figure 4: NMR spectra of the unknown solid (top) and ammonium nitrate standard (bottom). The left plots show the fine structure splitting of the ammonium ion, while the right plots show the hyperfine structure due to protium-deuterium coupling.

The left plots in figure 4 show the acquired proton NMR spectra of the unknown (top) and ammonium nitrate standard (bottom). Since ammonium is a highly symmetric molecule the proton spins ($^1$H = ½) will couple to the spin of the nitrogen atom ($^{14}$N = 1), splitting the energy levels and resulting in a triplet system with each peak having equal intensity. Therefore, the proton peaks shown in figure 4 (left) are characteristic of an ammonium ion. The proton shifts are also consistent with reported literature values.[36–42]

Further characterization can be achieved by examining the hyperfine structure of one of the triplet peaks as shown in figure 4 (right). Since the unknown and ammonium nitrate standard both contain a natural abundance of hydrogen, they both will be composed overwhelmingly of the protium hydrogen isotope. However, since the ammonium ion is acidic and was dissolved in $D_2O$, chemical exchange will occur between these two molecules. As a result, there will be a mixture of ammonium ions, each possessing a different fraction of protium and deuterium isotopes. Since this generates a slightly altered chemical environment with species possessing different nuclear spins, there will be spin coupling between the protium isotopes and deuterium isotopes, with each



Air Force Office of Scientific Research Grant FA9550-18-1-0442

resulting in a different spin splitting system. The molecule $NHD_3^+$ ion yields a septet system, $NH_2D_2^+$ yields a pentet system, $NH_3D^+$ yields a triplet system, and the $NH_4^+$ yields a singlet system.[36,39] This hyperfine splitting is highlighted in the ammonium nitrate standard in figure 4 (bottom-right). The unknown also displays the expected splitting, although, the acquired spectra was broadened, making the finer peaks difficult to resolve. This broadening is likely due to a combination of concentration effects and a less than optimal magnetic alignment (shim). Regardless, both plots display the characteristic spectral features expected from $NH_4^+$.

From analysis of the NMR spectra and comparison with the ammonium nitrate standard and spectra reported in the literature, it can be concluded with high confidence that the unknown solid is composed of an ammonium ion, consistent with the pH analysis.

## FOURIER TRANSFORM INFRARED SPECTROSCOPY

Final analysis of the unknown solid was accomplished utilizing Fourier transform infrared (FT-IR) spectroscopy. A small sample of the unknown solid was mixed with potassium bromide (KBr) and formed into a pellet for analysis. The same procedure was used for the preparation of an ammonium nitrate standard pellet. The FT-IR spectrometer that was used possesses a resolution of 4.0 $cm^{-1}$ and was background corrected prior to the acquisition of spectra. The resulting transmission data were converted into absorbance spectra ($log_{10}$) and are shown in figure 5. A simple visual comparison between these two acquired spectra conclusively demonstrates the unknown solid is composed of ammonium nitrate.

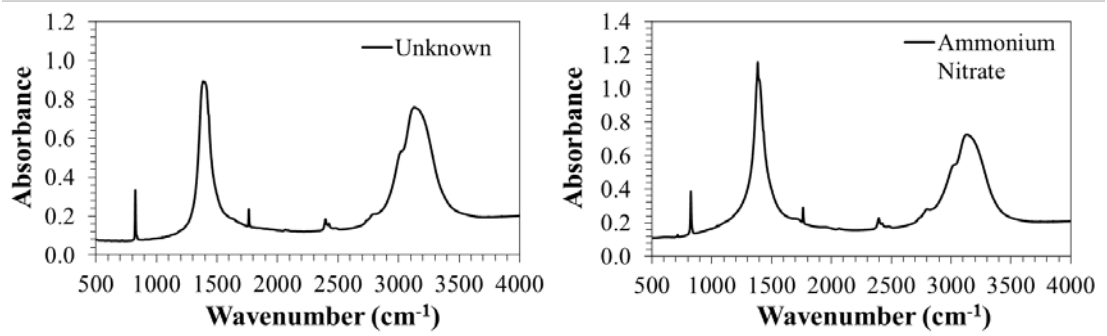


Figure 5: FT-IR analysis of the unknown solid (left) and an ammonium nitrate standard (right).

## ASSESSMENT OF THE SPECTROSCOPIC ANALYSIS

From analysis of the Raman spectra, NMR spectra, FT-IR spectra, and pH measurements, we can conclude with a high level of confidence that the unknown white solid generated from the decomposition of HAN is ammonium nitrate which is subsequently deposited onto the surface of the cool quartz tube. It should be noted that the white solid collected was conclusively shown to be ammonium nitrate specifically for the temperature and flow rate utilized for this initial experiment, as will be discussed below, changes to the temperature and/or flow rate can alter the chemical composition of this white solid, resulting in a binary mixture of salt species.

## QUANTIFICATION OF $NH_3$ AND $HNO_3$

As discussed, the thermal decomposition of HAN is predicted to yield the formation of ammonia and nitric acid as detailed in R1-R6. It has now been shown that the formation of these species in the gas phase are subsequently deposited on the cool surface of the quartz tube. A comprehensive spectroscopic analysis of the deposited solid conclusively showed that the substance formed was ammonium nitrate.

The stoichiometry for the overall reaction, R6, suggests that ammonia is expected to be the limiting reagent in the formation of ammonium nitrate, with nitric acid being the excess



Air Force Office of Scientific Research Grant FA9550-18-1-0442

reagent. Therefore, quantifying the amount of ammonium nitrate collected can be directly related to the amount of ammonia produced from the thermal decomposition process. Finally, since the experimental system allows for controlled amounts of HAN to be delivered to the thermal decomposition system, the amount of ammonia produced can be directly related to the amount of injected HAN.

## ESTIMATING % RECOVERY OF THE SYSTEM

The quantification of ammonia and nitric acid is predicated on the ability to collect and measure the amount of ammonium nitrate collected on the cool surface of the quartz tube. Therefore, it was necessary to determine the efficiency of the collection and detection system. This was accomplished by injecting known quantities of an aqueous nitric acid solution into the thermal decomposition system. Additionally, ammonia vapor, produced from the headspace of a sealed flask containing a solution of ammonium hydroxide, was introduced into the system through a heated leak valve. The combination of these two species simulates in a controlled way the expected generation and deposition of ammonium nitrate from the decomposition of HAN.

For these experiments a 2.62 M nitric acid solution was injected into the thermal decomposition system set to a temperature of 450 K. The flow rate utilized for this study was 83 nL/s with an injection time of 20 minutes. Upon completion of the 20-minute injection time, the system was brought to atmosphere, and the quartz tube was removed. The resulting solid material on the tube was collected by depositing approximately 1 mL of water onto the inside of the tube while held level with the ground. The tube was then slowly rolled and tilted in a manner that allowed the pool of water to roll across the inner surface of the plasma tube, efficiently dissolving any solid salt material deposited. The pool of water was collected in a 7 mL glass vial and the process was repeated for a total of three rinsing's. Additional water was added to each vial for a total of ~7.0 g of solution. These solutions were then analyzed by Raman spectroscopy. Analytical standards of ammonium nitrate were prepared to generate a calibration curve which was used for quantification.

The process described above was repeated for several partial pressures of ammonia introduced into the system. Results shown in figure 6 represent the percent recovery of nitric acid injected into the system. Based on these results, at partial pressures above ~10 mTorr, ammonia becomes the excess reagent and yeilds a system recovery of ~98%.

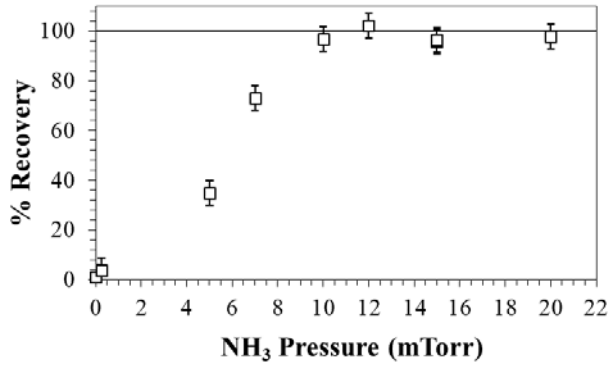


Figure 6: Percent recovery of nitric acid.

## HAN THERMAL DECOMPOSITON: PRODUCTION OF $NH_3$

### Temperature and Flow Rate Dependence: Partial vs Total Decomposition of HAN

The experimental system described above was designed to simulate the flow and injection of HAN into a decomposition system, generating species for subsequent gas-phase



Air Force Office of Scientific Research Grant FA9550-18-1-0442

ionization. Yet, the decomposition of HAN is not instantons and will depend on the kinetics of the system; thus, the degree to which HAN decomposes is dependent on both the temperature and duration within the thermal capillary prior to being vaporized. Therefore, the dynamic nature of the experimental configuration implies that certain operating conditions will result in only partial decomposition of HAN. Experiments were conducted by flowing HAN through the thermal decomposition system under controlled temperatures and flow rates. For each set of experimental conditions, the material deposited on the quartz tube was collected with water and stored in a glass vial as described previously.

Under conditions of partial HAN decomposition, the material deposited on the surface of the quartz tube is expected to be a combination of HAN and ammonium nitrate. Fortunately, Raman spectroscopy provides the ability to quantify the degree to which HAN is thermally decomposed. This is achieved by examining the ratio between the N-OH HAN peak at 1035.5 $cm^{-1}$ and the nitrate ion peak at 1076.6 $cm^{-1}$ which represents the combination of HAN and ammonium nitrate. To highlight this, Raman spectra of collected material for two temperatures at a constant flow rate are shown in figure 7. Under low temperature conditions the characteristic N-OH vibrational mode of HAN is clearly present, while the $NO_3^-$ symmetric stretching mode at 1076.6 $cm^{-1}$ is representative of both HAN and ammonium nitrate. Under high temperature conditions, the signature HAN peak at 1035.5 $cm^{-1}$ is no longer detectable, indicating HAN has undergone complete decomposition. The complete temperature and flow rate dependence of this analysis is shown in figure 7 (right). The relative ratio of these two Raman lines for HAN not subject to decomposition was found to be 0.195 and is represented by the dashed line in figure 7 (right). Understandably, higher flow rates result in shorter residence times within the heated capillary; thus, higher temperatures are required in order to achieved the same level of thermal decomposition.

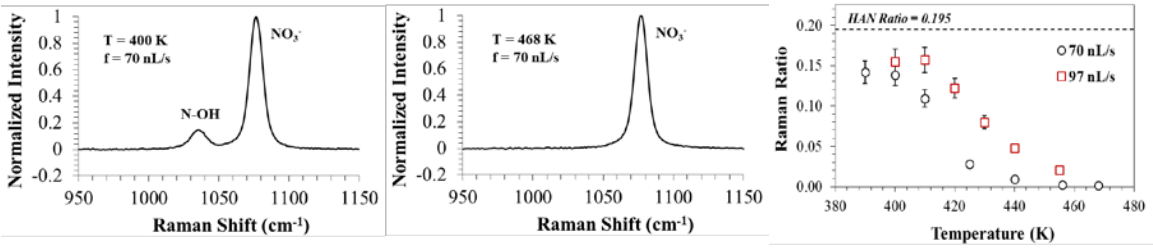


Figure 7: Raman spectra at 400 K (left), Raman spectra at 468 K (middle), and Raman ratio comparing the 1035.5 $cm^{-1}$ HAN line to the 1076.6 $cm^{-1}$ nitrate ion line (right).

## Temperature and Flow Rate Dependence: Quantifying $NH_3$

The data shown in figure 7 clearly indicates the presence of HAN under certain experimental conditions. In order to quantify the amount of ammonia produced from the collected ammonium nitrate, the contribution of HAN to the 1076.6 $cm^{-1}$ Raman signal must be accounted for. Fortunately, we can utilize the Raman signal at 1035.5 $cm^{-1}$, which is representative of the N-OH vibrational mode of HAN. Analytical standards of HAN were prepared in order to generate a calibration curve, which was then used to quantify the amount of HAN collected on the quartz tube. Similarly, analytical standards of ammonium nitrate were prepared in order to quantify the amount of nitrate ion collected. Therefore, we are able to subtract the contribution of HAN from the 1076.6 $cm^{-1}$ signal, resulting in the quantification of ammonia collected for a set of experimental conditions. Results on the quantification of ammonia generated relative to the amount of HAN injected during the decomposition process is shown in figure 8. As expected, increasing the temperature increases the degree to which HAN is thermally decomposed; thus, more ammonia is produced, and the ratio begins to approach 0.5, consistent with R6. Although, interestingly, the lower flow rate produced a lower yield of ammonia. A possible explanation for this observation may be that longer residence times within the heated capillary result in additional decomposition reactions that kinetically compete with the production of ammonia. For example, Oxley and Brower examined the thermal decomposition of HAN mixed with a small quantity of isotopically labeled ammonium nitrate, $^{15}NH_4NO_3$, at a temperature of 403 K (130 °C).[23] Isotopic



Air Force Office of Scientific Research Grant FA9550-18-1-0442

analysis allowed them to conclude that a small portion of ammonium ion, $^{15}NH_4^+$, was converted to dinitrogen, $N_2$. Further investigation of this result is required in order to provide a more substantial conclusion to the results shown in figure 8.

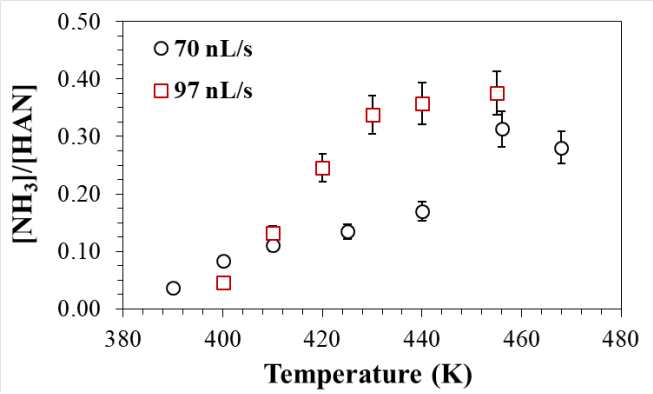


Figure 8: Amount of ammonia generated from HAN decomposition relative to amount of HAN injected.

## HAN THERMAL DECOMPOSITON: PRODUCTION OF $HNO_3$

The detection of gas phase nitric acid is not trivial. Mass spectrometry could be utilized; however, the ionization method that is used determines the sensitivity of the detection methodology. Hard ionization methods such as electron impact ionization result in a near complete fragmentation of the molecular form of nitric acid. Recently, it has been proposed that utilizing low electron energies could offset some of the loss incurred due to fragmentation and allow detection of the molecular ion form of nitric acid, $HNO_3^+$, at m/z = 63.[32] Initially we explored this possibility by injecting nitric acid into the system and observing the $HNO_3^+$ mass. Figure 9 shows the m/z = 63 signal dependence on the electron ionization energy. These results indicate that a low electron energy may reduce the degree at which nitric acid is fragmented; however, it also reduces the degree at which it is ionized, yielding a net lower signal. Furthermore, the data shown in figure 9 were from a 6.896 M aqueous nitric acid solution while concentrations below ~3 M yielded no observable signal regardless of experimental conditions. From R1 [HAN] = [$HNO_3$] = 2.8 M, therefore, the molecular ion at m/z = 63 could not be utilized for the detection and quantification of nitric acid. Even if higher concentrations of HAN were to be utilized, the use of the $HNO_3^+$ at m/z = 63 is not be recommended due to its demonstrated poor sensitivity. The use of mass spectrometry may be possible if a softer ionization method were to be utilized such as resonant photo-ionization; however, this would need to be experimentally confirmed.

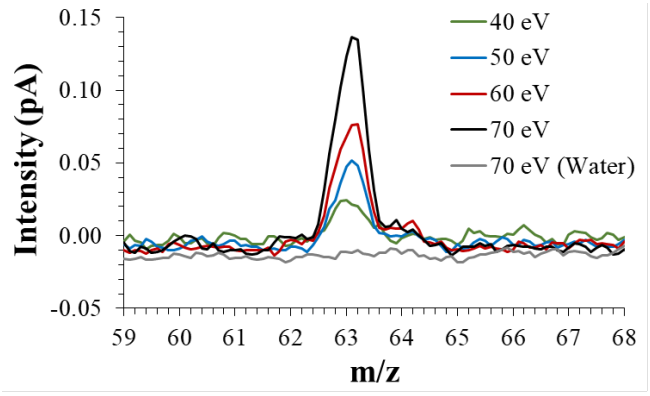


Figure 9: Mass spectrum of nitric acid molecular ion, m/z = 63, for various electron impact energies. A 6.89 M aqueous nitric acid solution was vaporized at a temperature of 400 K.



Air Force Office of Scientific Research Grant FA9550-18-1-0442

It is common practice in mass spectrometry to utilize the most abundant ion produced from the ionization source, which is often an ionized fragment rather than the molecular form of the species of interest, for measurement. In the case of nitric acid, fragments of nitric oxide ($NO^+$, m/z = 30) and nitrogen dioxide ($NO_2^+$, m/z = 46) are prevalent and easily detected with the current mass spectrometer. Unfortunately, as shown in the overall reaction, R6, HAN is predicted to produce nitroxyl (HNO) which almost completely fragments into $NO^+$, providing a spectral interference at m/z = 30. It may be possible to utilize the m/z = 46 fragment of $HNO_3$, however, the production of $NO_2$ containing species from the thermal decomposition of HAN presents a challenge that would require further investigation. Exploring this possibility is currently under development.

A solution to the quantification of nitric acid given our current experimental configuration can be found with simple chemistry. As noted previously, stoichiometry predicts that ammonia will likely be the limiting reagent in the formation of ammonium nitrate; thus, the amount of ammonium nitrate collected is reflective of the amount of ammonia generated from the decomposition of HAN. However, if an excess of ammonia gas were introduced into the system, as was accomplished in the % recovery experiments described above, then the vaporized nitric acid would become the limiting reagent with ammonia being the excess reagent. Therefore, the amount of ammonium nitrate collected would now be representative of the quantity of nitric acid vaporized from the thermal decomposition of HAN.

The quantification of nitric acid generated from the thermal decomposition of HAN was carried out by supplying ammonia gas through a heated leak valve into the decomposition system. An ammonia partial pressure of 50 mTorr was utilized for these experiments so that ammonia was present in large excess (see figure 6). The solid material collected was stored in glass vials for Raman analysis, as described previously. Results from these experiments can be seen in figure 10.

From the results shown in figure 10, we see that at low temperatures most of the nitric acid is unreacted and allowed to form ammonium nitrate. As the temperature increases, the amount of nitric acid, relative to the amount of HAN injected, decreases. Due to the lack of dependence on the flow rate of nitric acid introduced into the decomposition system, it seems unlikely that chemical reactions are responsible for the removal of nitric acid. Exploring this result is the focus of ongoing work.

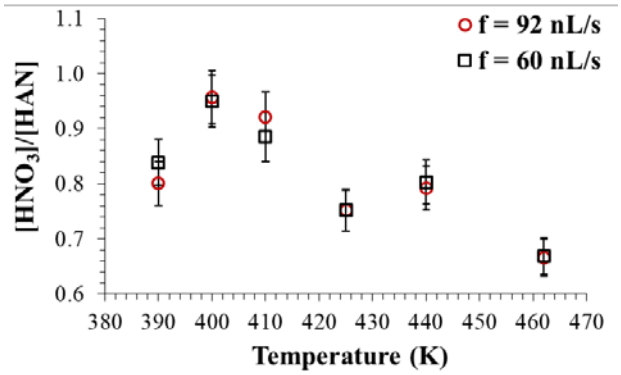


Figure 10: Amount of $HNO_3$ generated from HAN decomposition relative to amount of HAN injected.

## SUMMARY AND CONCLUSIONS

We have designed an experimental system that examines the generation of ammonia and nitric acid from the thermal decomposition of HAN. This has been achieved by condensing the generated material onto a quartz tube in the form of ammonium nitrate. A complete spectroscopic analysis of this solid material confirmed it to be pure ammonium nitrate when operated under low flow rate and high temperature conditions. However, Raman analysis



Air Force Office of Scientific Research Grant FA9550-18-1-0442

confirmed that HAN undergoes only partial thermal decomposition, with the degree of decomposition dictated by the flow rate and temperature. As the temperature of the decomposition system is increased, the amount of ammonia produced relative to the amount of HAN introduced concurrently increases, with both flow rates examined approaching the stoichiometrically predicted value of 0.5. Deviations from the value of 0.5 can be explained by losses that occur do to competing decomposition reaction mechanisms.

Nitric acid was quantitatively determined in a similar fashion to that of ammonia. Excess ammonia vapor introduced into the system allowed all vaporized nitric acid to be converted into ammonium nitrate, which was directly related to the amount of nitric acid vaporized. The low temperature regime showed values close to 1 indicating that most of the nitric acid was simply vaporized and collected in the form of condensed ammonium nitrate. However, increasing the temperature caused the amount of nitric acid collected to decrease. The lack of dependence on the flow rate at which HAN is introduced suggests that chemical reactions are not responsible for the decrease in vaporized $HNO_3$. Exploring this result is the focus of ongoing work.

## ACKNOWLEDGMENTS

This work was supported by the Air Force Office of Scientific Research Grant FA9550-18-1-0442.

## REFERENCES


1. Donius, B. R. & Rovey, J. L. Ionic Liquid Dual-Mode Spacecraft Propulsion Assessment. *J. Spacecr. Rockets* **48**, 110–123 (2011).
2. Donius, B. R., Rovey, J. L., Propulsion, C., Agency, I., Nitrate, H., Red, I., Nitric, F., Impulse, S., Tertroxide, N., Pressure, C. C., Dimethylhydrazine, U., Fuming, W., Acid, N. & Hall, T. Analysis and Prediction of Dual-Mode Chemical and Electric Ionic Liquid Propulsion Performance. in *48th AIAA Aerospace Sciences Meeting* AIAA-2010-1328 (2010).
3. Lozano, P., Glass, B. & Martinez-Sanchez, M. Performance characteristics of a linear ionic liquid electrospray thruster. in *29th International Electric Propulsion Conference* IEPC-2005-192 (2005).
4. Lozano, P. & Martinez-sanchez, M. Efficiency Estimation of EMI-BF4 Ionic Liquid Electrospray Thrusters. in *41st AIAA/ASME/SAE/ASEE Joint Propulsion Conference* AIAA-2005-4388 (2005).
5. Lozano, P. & Martínez-Sánchez, M. Ionic liquid ion sources: Suppression of electrochemical reactions using voltage alternation. *J. Colloid Interface Sci.* **280**, 149–154 (2004).
6. Courtney, D. G., Dandavino, S. & Shea, H. Comparing direct and indirect thrust measurements from passively fed ionic electrospray thrusters. *J. Propuls. Power* **32**, 392–407 (2016).
7. Gomez Jenkins, M., Krejci, D. & Lozano, P. CubeSat constellation management using Ionic Liquid Electrospray Propulsion. *Acta Astronaut.* **151**, 243–252 (2018).
8. Lozano, P. C., Martínez-Sánchez, M. & Hruby, V. Electrospray Propulsion. *Encycl. Aerosp. Eng.* 1–12 (2010) doi:10.1002/9780470686652.eae121.
9. Zorzos, A. N. & Lozano, P. C. The use of ionic liquid ion sources in focused ion beam applications. *J. Vac. Sci. Technol. B Microelectron. Nanom. Struct.* **26**, 2097 (2008).
10. Garoz, D., Bueno, C., Larriba, C., Castro, S., Romero-Sanz, I., Fernandez de la Mora, J., Yoshida, Y. & Saito, G. Taylor cones of ionic liquids from capillary tubes as sources of pure ions: The role of surface tension and electrical conductivity. *J. Appl. Phys.* **102**, 064913 (2007).
11. Romero-Sanz, I., Aguirre De Carcer, I. & Fernandez De La Mora, J. Ionic propulsion based on heated Taylor cones of ionic liquids. *J. Propuls. Power* **21**, 239–242 (2005).
12. Romero-Sanz, I., Bocanegra, R., Fernandez de la Mora, J. & Gamero-Castaño, M. Source of heavy molecular ions based on Taylor cones of ionic liquids operating in the pure ion evaporation regime. *J. Appl. Phys.* **94**, 3599–3605 (2003).
13. Shamshina, J. L., Smiglak, M., Drab, D. M., Parker, T. G., Dykes, H. W. H., Di Salvo, R., Reich, A. J. & Rogers, R. D. Catalytic ignition of ionic liquids for propellant applications. *Chem. Commun.* **46**, 8965–7 (2010).
14. Oommen, C., Rajaraman, S., Chandru, R. A. & Rajeev, R. Catalytic Decomposition of Hydroxylammonium Nitrate Monopropellant. *Proc. Int. Conf. Chem. Chem. Process (ICCCP 2011)* **10**, 205–209 (2011).
15. Jankovsky, R. S. Han-based monopropellant assessment for spacecraft. *32nd Jt. Propuls. Conf. Exhib.* (1996) doi:10.2514/6.1996-2863.
16. Farshchi, M., Vaezi, V. & Shaw, B. D. Studies of Han-based monopropellant droplet combustion. *Combust. Sci. Technol.* **174**, 71–97 (2002).
17. Courthéoux, L., Amariei, D., Rossignol, S. & Kappenstein, C. Thermal and catalytic decomposition of HNF and HAN liquid ionic as propellants. *Appl. Catal. B Environ.* **62**, 217–225 (2006).
18. Khare, P., Yang, V., Meng, H., Risha, G. A. & Yetter, R. A. Thermal and electrolytic decomposition and ignition of han-water solutions. *Combust. Sci. Technol.* **187**, 1065–1078 (2015).
19. Lee, H. S. & Litzinger, T. A. Thermal decomposition of han-based liquid propellants. *Combust. Flame* **127**, 2205–2222 (2001).




Air Force Office of Scientific Research Grant FA9550-18-1-0442

20. Lee, H. S. & Litzinger, T. A. Chemical kinetic study of HAN decomposition. *Combust. Flame* (2003) doi:10.1016/S0010-2180(03)00157-3.
21. Lee, Y. J. & Litzinger, T. A. Combustion chemistry of HAN, TEAN, and XM46. *Combust. Sci. Technol.* **141**, 19–36 (1999).
22. Meng, H., Khare, P., Risha, G. A., Yetter, R. A. & Yang, V. Decomposition and ignition of HAN-based monopropellants by electrolysis. *47th AIAA Aerosp. Sci. Meet. Incl. New Horizons Forum Aerosp. Expo.* 1–16 (2009) doi:10.2514/6.2009-451.
23. Thermal_Decomposition_of_Hydroxylamine_Nitrate_Oxley&Brower.pdf.
24. Berg, S. P. & Rovey, J. L. Decomposition of Monopropellant Blends of Hydroxylammonium Nitrate and Imidazole-Based Ionic Liquid Fuels. *J. Propuls. Power* **29**, 125–135 (2013).
25. Zube, D. M., Wucherer, E. J. & Reed, B. Evaluation of HAN-Based Propellant Blends. in *39th AIAA/ASME/SAE/ASEE Joint Propulsion Converence* AIAA-2003-4643 (2003).
26. Kidd, F. G., Baird, M. J., Neff, G. & Lemmer, K. Experimental Vaporization and Computational Modeling of Ionization of Hydroxylammonium Nitrate in Vacuum. *34th Int. Electr. Propuls. Conf.* (2015).
27. Liu, L., Wei, C., Guo, Y., Rogers, W. J. & Sam Mannan, M. Hydroxylamine nitrate self-catalytic kinetics study with adiabatic calorimetry. *J. Hazard. Mater.* (2009) doi:10.1016/j.jhazmat.2008.06.009.
28. Liu, L., Papadaki, M., Pontiki, E., Stathi, P., Rogers, W. J. & Mannan, M. S. Isothermal decomposition of hydroxylamine and hydroxylamine nitrate in aqueous solutions in the temperature range 80-160 °C. *J. Hazard. Mater.* **165**, 573–578 (2009).
29. Farhat, K., Amariei, D., Batonneau, Y., Kappenstein, C. & Ford, M. Reaction balance of thermal and catalytic decomposition of nitrogen-based ionic monopropellants. *Collect. Tech. Pap. - 43rd AIAA/ASME/SAE/ASEE Jt. Propuls. Conf.* **6**, 6254–6263 (2007).
30. Wei, C., Rogers, W. J. & Mannan, M. S. Thermal decomposition hazard evaluation of hydroxylamine nitrate. in *Journal of Hazardous Materials* (2006). doi:10.1016/j.jhazmat.2005.07.044.
31. Cronin, J. T. & Brill, T. B. Thermal decomposition of energetic materials. 8. Evidence of an oscillating process during the high-rate thermolysis of hydroxylammonium nitrate, and comments on the interionic interactions. *J. Phys. Chem.* **90**, 178–181 (1986).
32. Chambreau, S. D., Popolan-Vaida, D. M., Vaghjiani, G. L. & Leone, S. R. Catalytic Decomposition of Hydroxylammonium Nitrate Ionic Liquid: Enhancement of NO Formation. *J. Phys. Chem. Lett.* **8**, 2126–2130 (2017).
33. Jonusas, M. & Krim, L. A possible answer to the mysterious non-detection of hydroxylamine in space: The thermal desorption mechanism. *Mon. Not. R. Astron. Soc.* **459**, 1977–1984 (2016).
34. Izato, Y. I., Koshi, M. & Miyake, A. Initial Decomposition Pathways of Aqueous Hydroxylamine Solutions. *J. Phys. Chem. B* **121**, 4502–4511 (2017).
35. Wang, Q., Wei, C., Pérez, L. M., Rogers, W. J., Hall, M. B. & Mannan, M. S. Thermal decomposition pathways of hydroxylamine: Theoretical investigation on the initial steps. *J. Phys. Chem. A* **114**, 9262–9269 (2010).
36. Perrin, C. L. & Engler, R. E. Secondary hydrogen/deuterium kinetic isotope effect of dissociation of aqueous ammonium ion. *J. Phys. Chem.* **95**, 8431–8433 (1991).
37. Emerson, M. T., Grunwald, E. & Kromhout, R. A. Proton-transfer studies by nuclear magnetic resonance. I. Diffusion control in the reaction of ammonium ion in aqueous acid. *J. Chem. Phys.* **33**, 547–555 (1960).
38. Fraenkel, G., Asahi, Y., Batiz-Hernandez, H. & Bernheim, R. A. Isotope shifts and spin coupling in the proton magnetic resonance of deuterated ammonium ions. *J. Chem. Phys.* **44**, 4647–4649 (1966).
39. Sanders, J. K. M., Hunter, B. K., Jameson, C. J. & Romeo, G. Isotope effects on proton chemical shifts and coupling constants in the ammonium ions 15, 14 NH4-nDn+. *Chem. Phys. Lett.* **143**, 471–476 (1988).
40. Wu, G., Cooks, R. G. & Ouyang, Z. Geometry optimization for the cylindrical ion trap: Field calculations, simulations and experiments. *Int. J. Mass Spectrom.* **241**, 119–132 (2005).



Air Force Office of Scientific Research Grant FA9550-18-1-0442

41. Mansour, M. S. & Chen, Y.-C. Line Raman, Rayleigh, and laser-induced predissociation fluorescence technique for combustion with a tunable KrF excimer laser. *Appl. Opt.* **35**, 4252–4260 (1996).
42. Bengtsson, L. A., Frostemark, F. & Holmberg, B. Speciation, Structural Characteristics and Proton Dynamics in the - Systems NH4NO3 1.5 H2O and NH4NO3 1.5 H2O - (HNO3, NH4F, NH3)-H2O at 50 C. **90**, 559–570 (1994).



Air Force Office of Scientific Research Grant FA9550-18-1-0442